3D Plasma Equilibrium and Stability with Hot Particle Pressure Anisotropy

W. A. Cooper[1], J. P. Graves[1], S. P. Hirshman[2], P. Merkel[3], J. Kisslinger[3], H. F. G. Wobig[3], K. Y. Watanabe[4] and Y. Narushima[4]

[1]Ecole Polytechnique Fédérale de Lausanne (EPFL), Association EURATOM-Confédération Suisse, Centre de Recherches en Physique des Plasmas, CH1015 Lausanne, Switzerland.

[2]Fusion Energy Division, Oak Ridge National Laboratory, Oak Ridge, TN, USA.

[3]Max Planck Institut für Plasmaphysik, Garching, Germany.

[4]National Institute for Fusion Science, Oroschi-cho 322-6, Toki 509-5292, Japan

Motivation and Background

- $10MW$ tangential neutral beam injection that yields $180kev$ energetic ions can drive large pressure anisotropy in LHD discharges. *(T. Yamaguchi et al., Nucl. Fusion* 45 *(2005) L33)*.
- ICRH in JET produces significant perpendicular pressure anisotropy that can be very accurately described with a Bi-Maxwellian distribution function for the energetic ions.*(J. P. Graves et al., Proc. Varenna-Lausanne International Workshop on Theory of Fusion Plasmas (2006) pp. 350-355)*.
- LHD has reported $\langle\beta\rangle \sim 5\%$ stable operation and may have thus surpassed ideal MHD stability predictions. *(Watanabe et al., Nucl. Fusion* 45 *(2005) 1247)*.

EXPERIMENTAL RESULTS IN THE LHD HELIOTRON

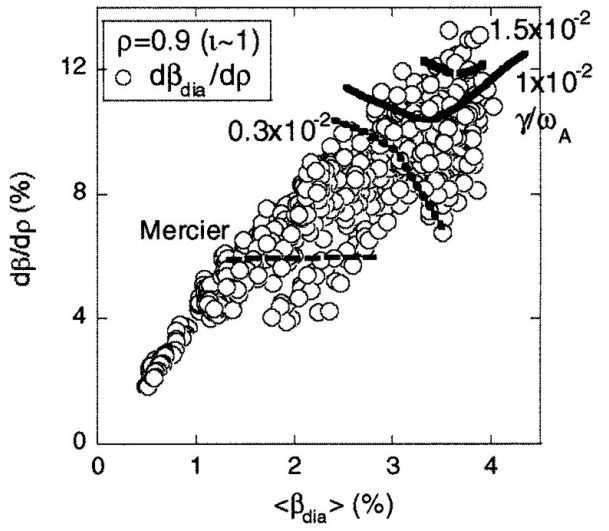

Figure 9. The beta gradients including the beam pressure are plotted over the contours of the low-n ideal MHD mode in figure 5.

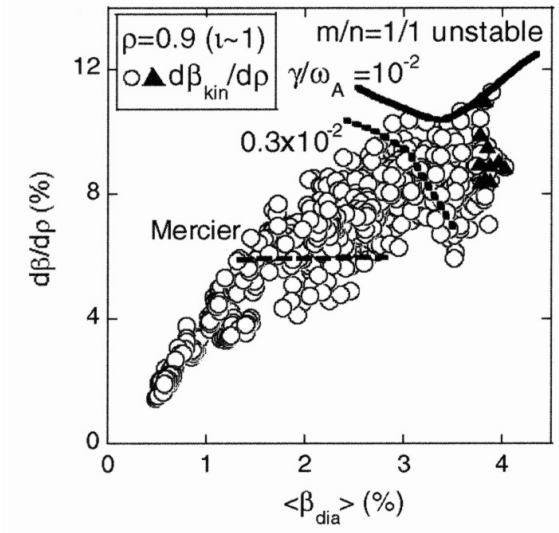

7. The thermal beta gradients are plotted over the contours ow-n ideal MHD mode in figure 5. The closed triangles ond to the high-beta discharge with $\langle\beta_{\rm dia}\rangle_{\rm max} = 4.0\%$ shown in figure 3.

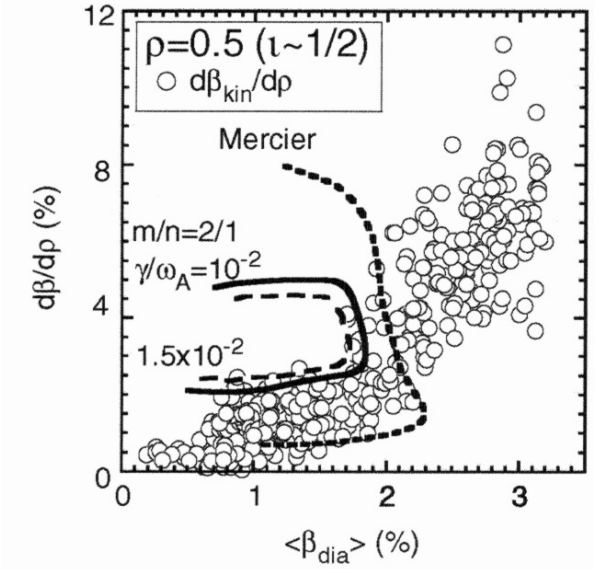

15. The observed thermal beta gradients at a core ratio surface, $\rho = 0.5(\iota \sim 0.5)$, in the standard configuration as a function of the beta value.

- The $m/n = 1/1$ exceeds the stability limits when the total pressure gradients of the experiment are compared with ideal MHD stability predictions.
- When only the thermal pressure gradients obtained in the experiment are plotted for the $m/n = 1/1$ and $m/n = 2/1$ modes, the stability curves show the data points to align with a marginal growth rate

Outline for Equilibrium Studies

- An equilibrium model based on a variant of a Bi-Maxwellian distribution that satisfies $\boldsymbol{B} \cdot \boldsymbol{\nabla} \mathcal{F}_h = 0$ can treat arbitrary anisotropy and energetic particle deposition.

- This Bi-Maxwellian model for hot particles has previously been successfully adapted to an old fixed boundary version of the VMEC code. (*W. A. Cooper et al., Nucl. Fusion* 46 *(2006) 683*.)

- The ANIMEC code has been developed in which this model is implemented in the most recent VMEC2000 free boundary version.

- Applications to a 2-period quasiaxisymmetric stellarator (QAS) have been investigated with off-axis high and low-field side energetic particle deposition to test the limits of the code.

Outline for Fluid Stability Studies

- Fluid magnetohydrodynamic stability models for anisotropic pressure plasmas have been implemented in the TERPSICHORE code *W. A. Cooper et al., Fusion Science & Technol.* 50 *(2006) 245*.
  Kruskal-Oberman energy principle $\Longrightarrow$ Fully interacting hot particles (KO).
  Johnson et al. energy principle $\Longrightarrow$ Rigid noninteracting hot particles (NI).

- Examine sequence of current-free fixed boundary LHD equilibria with vacuum $R_{ax} = 3.5m$ at fixed $\langle\beta_{dia}\rangle \sim 5\%$ and $\langle\beta_{th}\rangle \sim 3.5\%$ in the range $1/3 \leq T_{||}/T_{\perp} \leq 3$.

- Investigation of equilibrium and stability of beam driven fusion aspects in a Heliotron system.

Bi-Maxwellian Distribution Function

$$\mathcal{F}_h(s,\mathcal{E},\mu) = \mathcal{N}(s)\left(\frac{m_h}{2\pi T_\perp(s)}\right)^{3/2} \exp\left[-m_h\left(\frac{\mu B_c}{T_\perp(s)} + \frac{|\mathcal{E}-\mu B_c|}{T_{||}(s)}\right)\right]$$

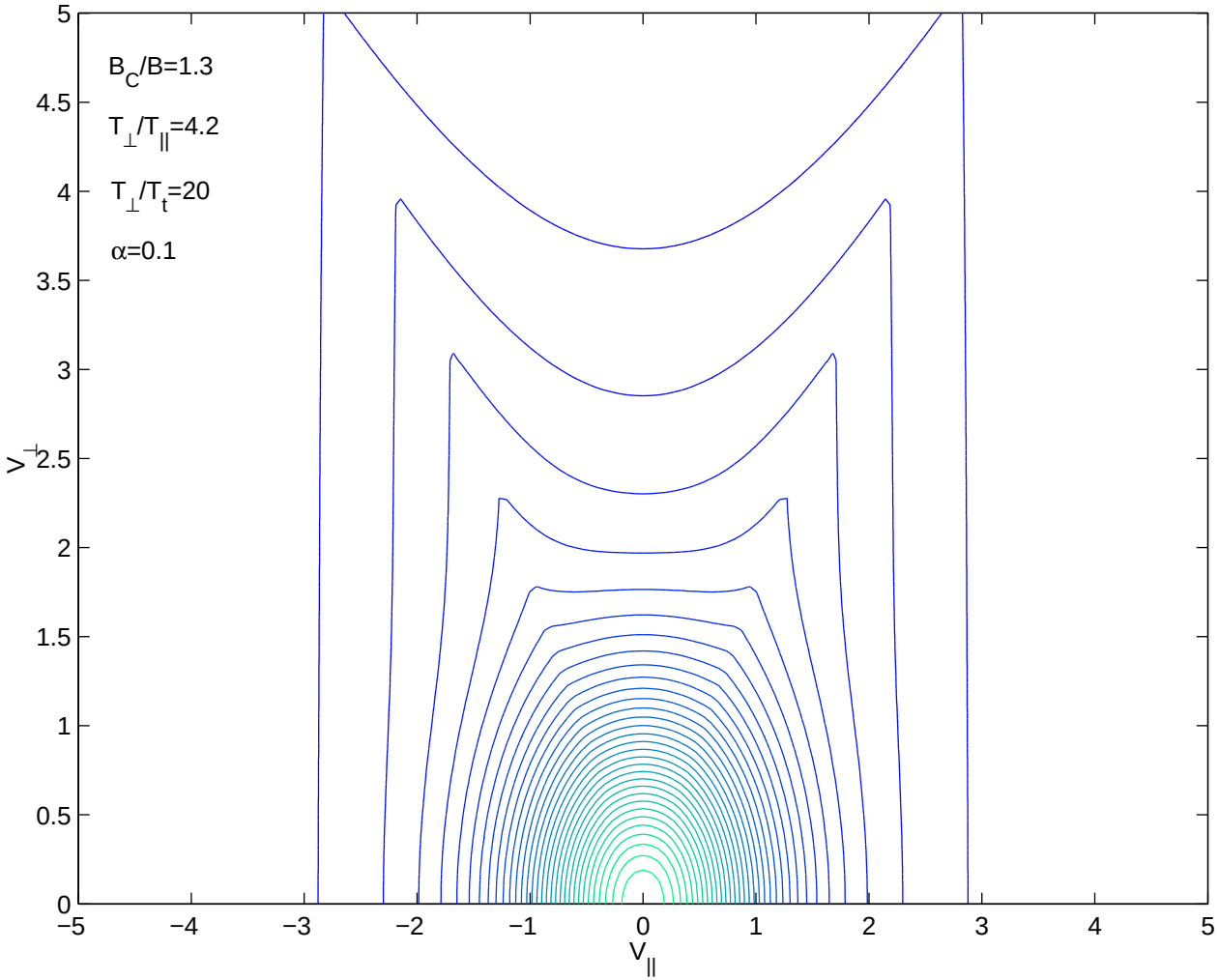

Bi-Maxwellian Pressure Moments

- Total parallel pressure

$$p_{\parallel}(s,B) = p(s) + \mathcal{N}(s) T_{\parallel}(s) H(s,B)$$

- FOR $B > B_C$:

$$H(s,B) = \frac{(B/B_C)}{\left[1 - \frac{T_\perp}{T_\parallel}\left(1 - \frac{B}{B_C}\right)\right]}$$

- FOR $B < B_C$:

$$H(s,B) = \frac{B}{B_C} \frac{\left[1 + \frac{T_\perp}{T_\parallel}\left(1 - \frac{B}{B_C}\right) - 2\left(\frac{T_\perp}{T_\parallel}\right)^{5/2}\left(1 - \frac{B}{B_C}\right)^{5/2}\right]}{\left[1 - \left(\frac{T_\perp}{T_\parallel}^2\right)\left(1 - \frac{B}{B_C}\right)^2\right]}$$

Equilibrium Relations

- $p_\perp$ DERIVED FROM PARALLEL FORCE BALANCE

$$p_\perp(s,B) = p_\parallel(s,B) - B\left.\frac{\partial p_\parallel}{\partial B}\right|_s$$

- FIREHOSE STABILITY CRITERION

$$\sigma \equiv \frac{1}{\mu_0} - \left.\frac{1}{B}\frac{\partial p_\parallel}{\partial B}\right|_s = \frac{1}{\mu_0} - \frac{p_\parallel - p_\perp}{B^2} > 0$$

- MIRROR STABILITY CRITERION

$$\tau \equiv \left.\frac{\partial(\sigma B)}{\partial B}\right|_s = \frac{1}{\mu_0} + \left.\frac{1}{B}\frac{\partial p_\perp}{\partial B}\right|_s > 0$$

VMEC Equilibrium Energy

$$W = \int\int\int d^3x \left(\frac{B^2}{2\mu_0} + \frac{p_{\|}(s,B)}{\Gamma - 1} \right)$$

$$p_{\|}(s,B) = M(s)[\Phi'(s)]^{\Gamma} \frac{1 + p_h(s)H(s,B)}{\langle 1 + p_h(s)H(s,B) \rangle^{\Gamma}}$$

- THE CHOICE $\mathcal{N}(s)T_{\|}(s) = p(s)p_h(s)$ RECONCILES THIS EXPRESSION WITH THE BI-MAXWELLIAN MOMENT.
- PROFILE CHOICES:
  - $p(s) = p(0)(1-s)(1-s^4)$,
  - $p_h(s) = p_h(0)s(1-s)$,
  - $2\pi J(s) = 0$,
  - $T_{\perp}/T_{||} = const.$,
  - Value of B_C determines hot particle deposition layer.
- GREEN'S FUNCTION TREATMENT OF VACUUM DOMAIN.

Flux surface averaged pressure profiles

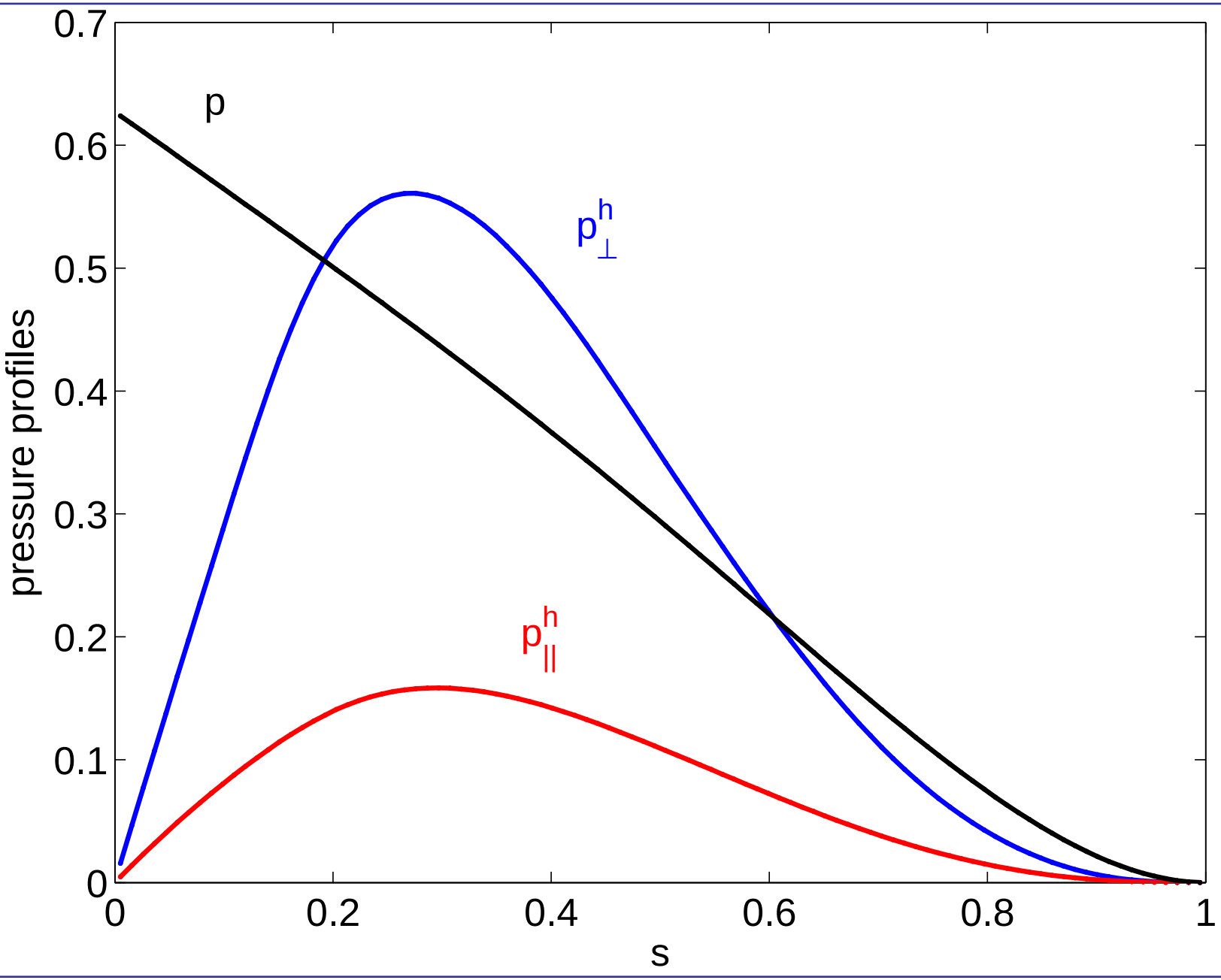

Application to 2-period quasiaxisymmetric stellarator reactor

- PARAMETERS:
  - $\langle \beta_{th} \rangle = \int\int\int d^3x 2\mu_0 p / \int\int\int d^3x B^2, \qquad \Gamma = 0$
  - $\langle \beta \rangle = \int\int\int d^3x \mu_0 [p_{\|} + p_{\perp}] / \int\int\int d^3x B^2,$

- Coils system and vacuum mod-B structure at plasma edge

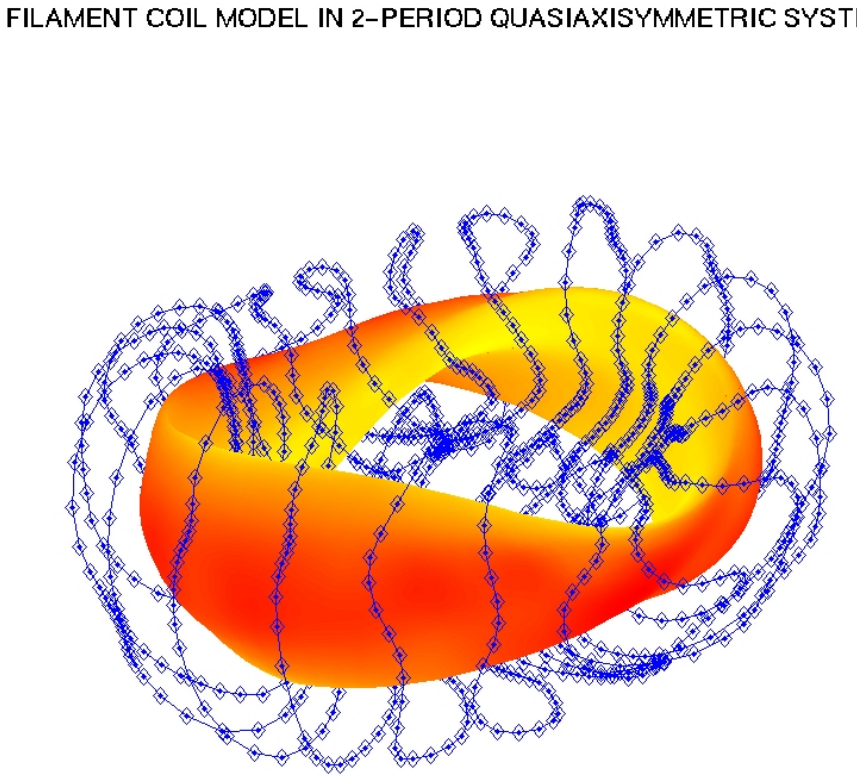

Vacuum quasiaxisymmetric stellarator flux surfaces

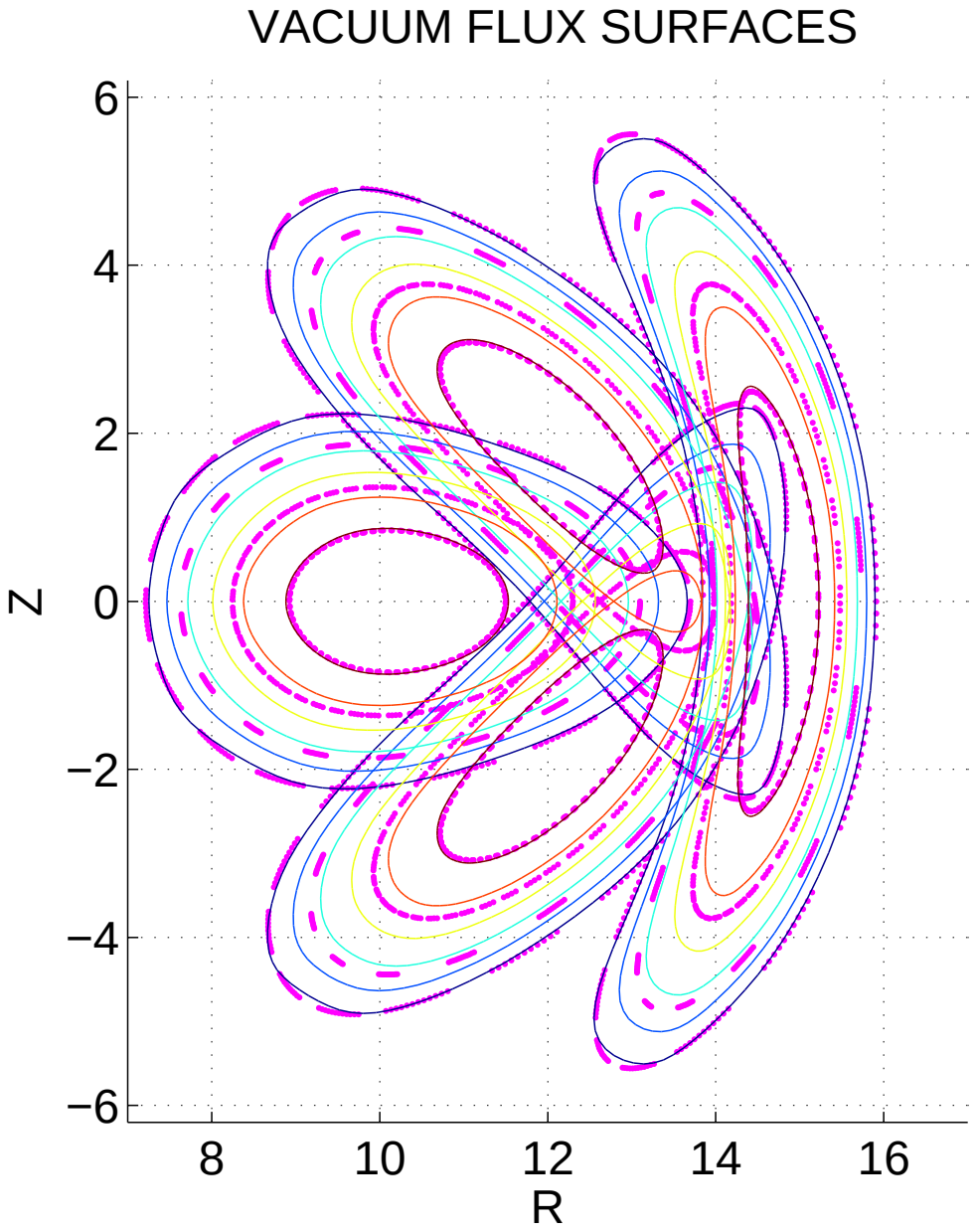

Diagnostics

- Force Balance

$$\boldsymbol{F} = -\frac{\partial p_{\|}}{\partial s}\bigg|_B \boldsymbol{\nabla} s + \boldsymbol{K} \times \boldsymbol{B}$$

- Surface Averaged Radial Force Balance

$$\left\langle \frac{F_s}{\Phi'(s)} \right\rangle = -\left\langle \frac{1}{\Phi'(s)} \frac{\partial p_{\|}}{\partial s}\bigg|_B \right\rangle - \frac{\partial}{\partial s}\left\langle \frac{\sigma B_v}{\sqrt{g}} \right\rangle - \iota(s) \frac{\partial}{\partial s}\left\langle \frac{\sigma B_u}{\sqrt{g}} \right\rangle$$

- Note that the total plasma current density is: $\boldsymbol{K} \equiv \boldsymbol{\nabla} \times (\sigma \boldsymbol{B})$

Flux surface averaged radial force balance (absolute values)

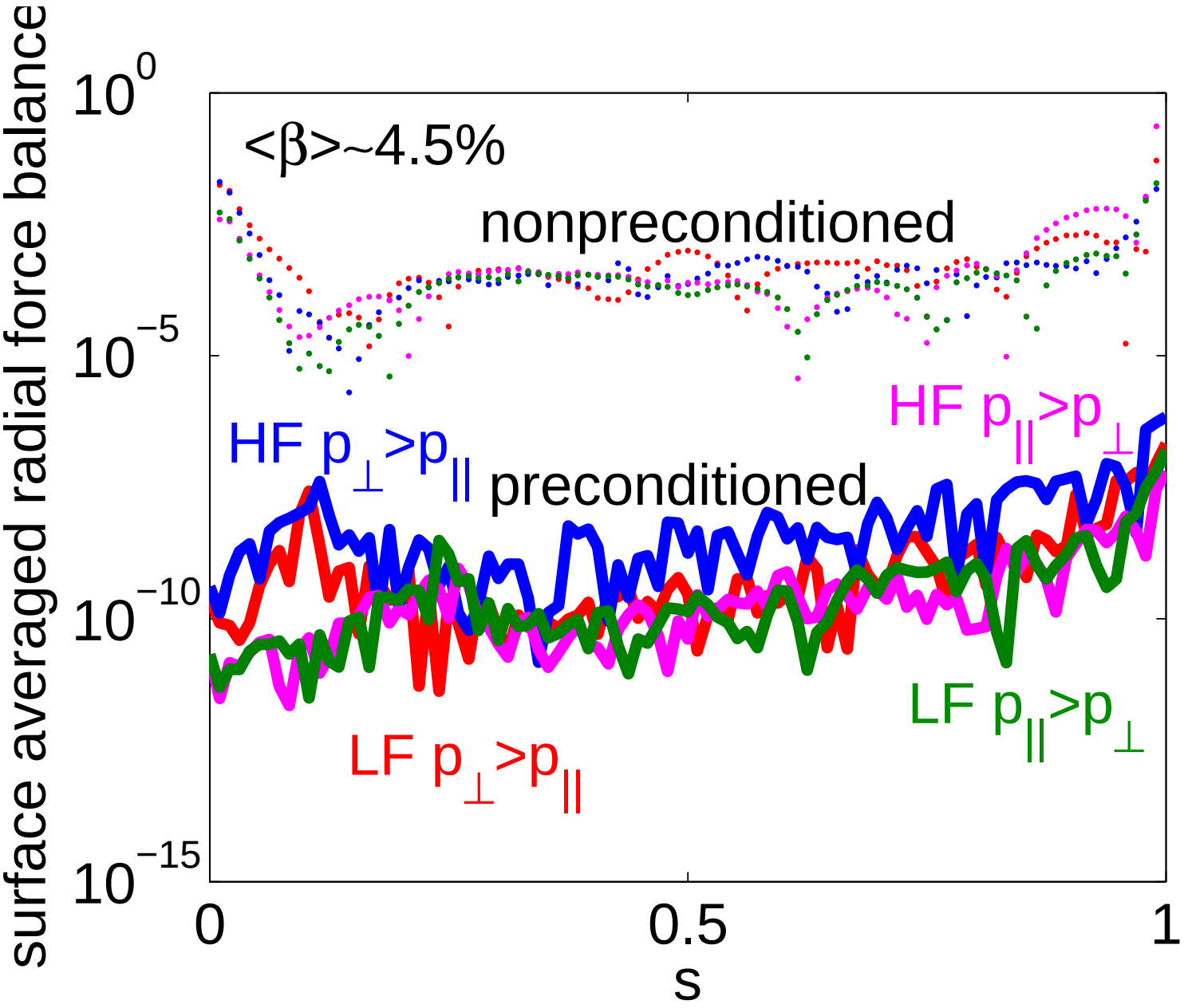

Hot particle pressure contours for $p_\perp > p_{||}$

HF

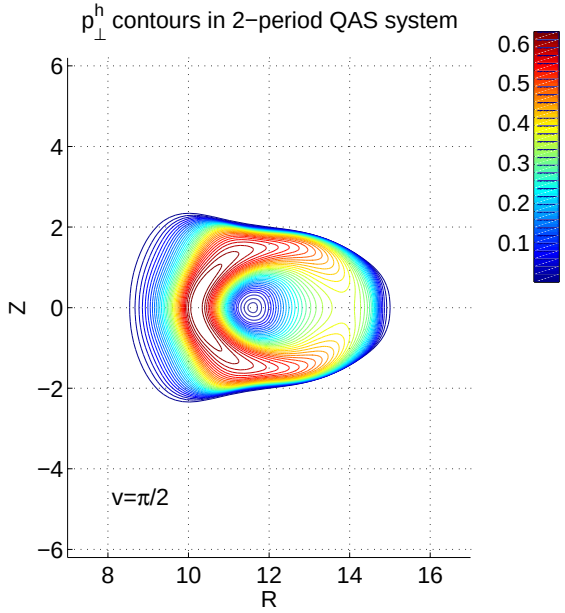

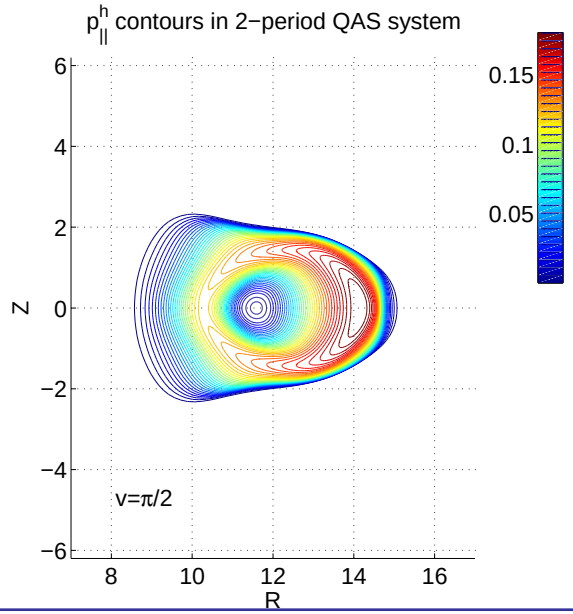

LF

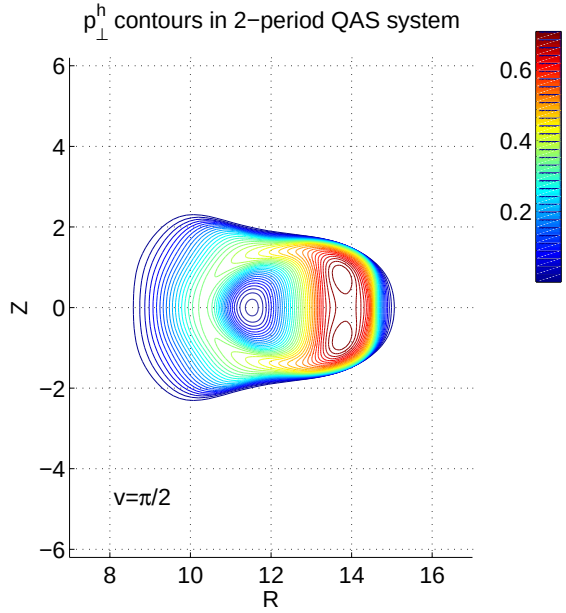

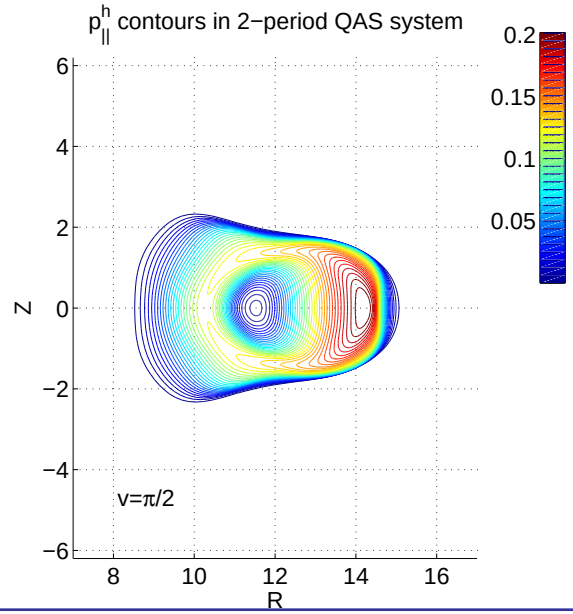

Hot particle pressure contours for $p_{||} > p_{\perp}$

HF

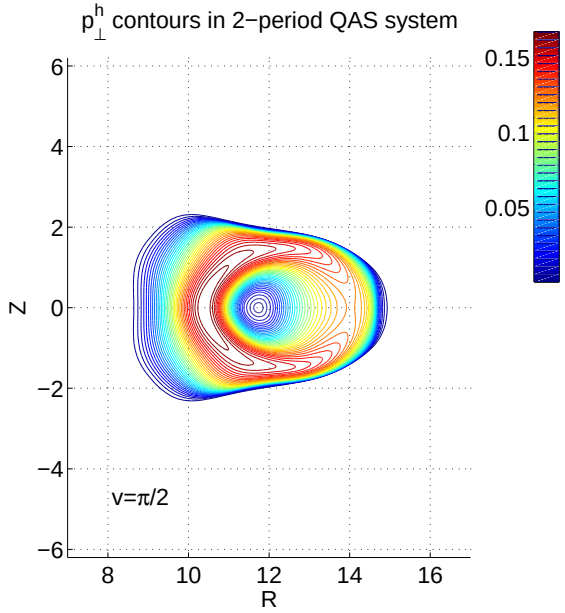

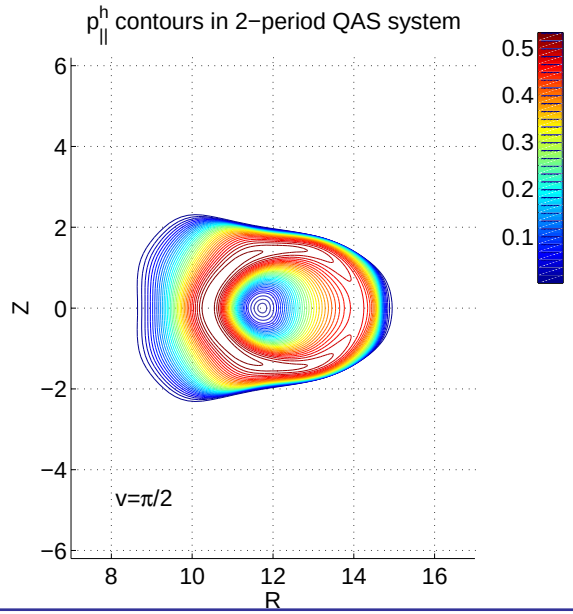

LF

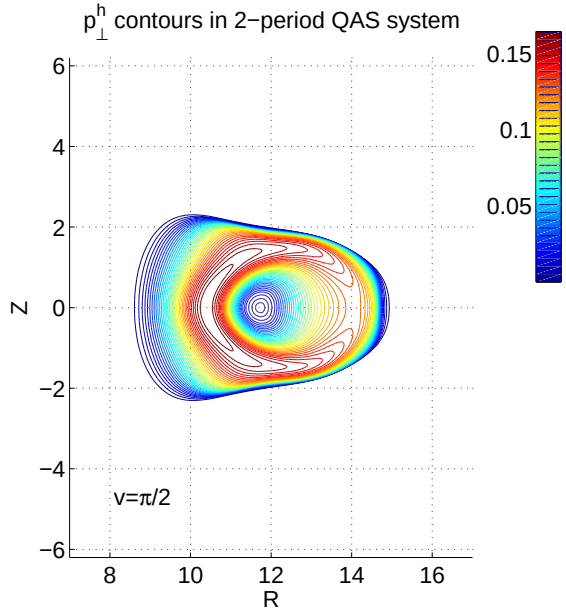

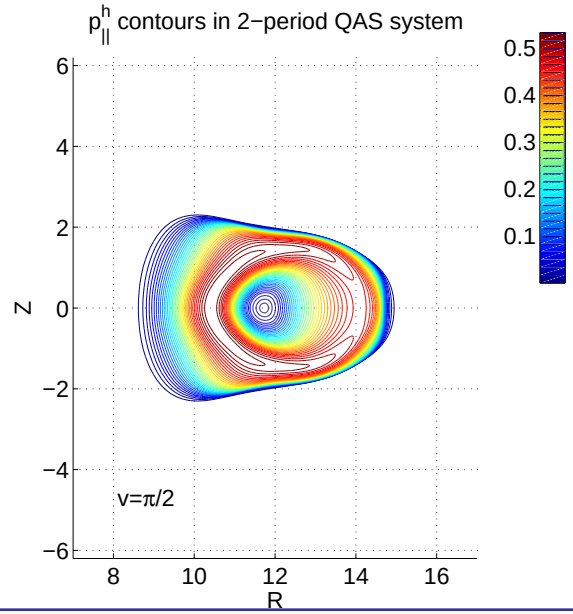

FLUID MHD STABILITY WITH THE TERPSICHORE CODE

- TWO ANISOTROPIC ENERGY PRINCIPLES IMPLEMENTED IN THE TERPSICHORE CODE ARE EXPLORED
  - The Kruskal-Oberman energy principle in which the thermal and the hot particle pressure gradients participate in the instability mechanisms. For $p_{||} = p_{\perp}$, the incompressible ideal MHD equations are recovered.
  - The rigid noninteracting hot particle energy principle of Johnson et al. in which the hot particle drift frequencies are ordered faster than the typical instability growth rates. In this case only the thermal particle pressure gradient and parallel current drive instabilities. All species, however, fully contribute to the equilibrium state.

- THE ENERGY PRINCIPLE

$$\langle \delta W_P \rangle + \langle \delta W_V \rangle - \omega^2 \langle \delta W_K \rangle = 0,$$
$$\langle \delta W_P \rangle = \langle \delta W_{C^2} \rangle + \langle \delta W_{BI} \rangle + \langle \delta W_J \rangle$$

THE BALLOONING-INTERCHANGE INSTABILITY DRIVE

- KRUSKAL-OBERMAN FULLY INTERACTING HOT PARTICLE MODEL

$$\delta W_{BI}(s) = -\frac{1}{2}\int_0^{\frac{2\pi}{L_s}} d\phi \int_0^{2\pi} d\theta \left(\frac{\tau}{\tau+\sigma}\right)\left(\frac{1}{\sigma B^2}\right)\left(\frac{\partial p_\parallel}{\partial s}\bigg|_B + \frac{\sigma}{\tau}\frac{\partial p_\perp}{\partial s}\bigg|_B\right)(\xi^s)^2 \times$$
$$\left[\sqrt{g}\left(\frac{\partial p_\parallel}{\partial s}\bigg|_B + \frac{\sigma}{\tau}\frac{\partial p_\perp}{\partial s}\bigg|_B\right) + \psi''(s)J(s) - \Phi''(s)I(s)\right.$$
$$\left. + \psi'(s)J'(s) - \Phi'(s)I'(s) + \sigma B_s(\boldsymbol{B}\cdot\boldsymbol{\nabla}\sqrt{g}) - \sigma B^2\frac{\partial\sqrt{g}}{\partial s}\right]$$

- JOHNSON et al. RIGID NONINTERACTING HOT PARTICLE MODEL

$$\delta W_{BI}(s) = -\frac{1}{2}\int_0^{\frac{2\pi}{L_s}} d\phi \int_0^{2\pi} d\theta \frac{p'(s)}{\sigma B^2}\left[\sqrt{g}\sigma p'(s) + \psi''(s)J(s) - \Phi''(s)I(s)\right.$$
$$\left. - \sigma B^2\frac{\partial\sqrt{g}}{\partial s}\right](\xi^s)^2 + \frac{1}{2}\int_0^{\frac{2\pi}{L_s}} d\phi \int_0^{2\pi} d\theta \left[\frac{p'(s)B_s}{B^2}\right]\sqrt{g}\boldsymbol{B}\cdot\boldsymbol{\nabla}(\xi^s)^2$$

THE GLOBAL KINK MODE INSTABILITY DRIVE

- KRUSKAL-OBERMAN FULLY INTERACTING HOT PARTICLE MODEL

$$\begin{aligned}\delta W_J(s) &= -\frac{1}{2}\int_0^{\frac{2\pi}{L_s}} d\phi \int_0^{2\pi} d\theta \frac{\boldsymbol{K}\cdot\boldsymbol{B}}{B^2}\Big[\frac{\sqrt{g}B^2}{\sigma|\boldsymbol{\nabla}s|^2}\Big(\frac{\boldsymbol{K}\cdot\boldsymbol{B}}{B^2}\Big) \\ &\quad +\psi'(s)\Phi''(s)-\Phi'(s)\psi''(s)\Big](\xi^s)^2 \\ &\quad -\frac{1}{2}\int_0^{\frac{2\pi}{L_s}} d\phi \int_0^{2\pi} d\theta \frac{\boldsymbol{K}\cdot\boldsymbol{B}}{B^2} h_s\sqrt{g}\boldsymbol{B}\cdot\boldsymbol{\nabla}(\xi^s)^2\end{aligned}$$

- JOHNSON et al. RIGID NONINTERACTING HOT PARTICLE MODEL

$$\begin{aligned}\delta W_J(s) &= -\frac{1}{2}\int_0^{\frac{2\pi}{L_s}} d\phi \int_0^{2\pi} d\theta \frac{\boldsymbol{j_p}\cdot\boldsymbol{B}}{B^2}\Big[\frac{\sqrt{g}B^2}{|\boldsymbol{\nabla}s|^2}\Big(\frac{\boldsymbol{j_p}\cdot\boldsymbol{B}}{B^2}\Big) \\ &\quad +\psi'(s)\Phi''(s)-\Phi'(s)\psi''(s)\Big](\xi^s)^2 \\ &\quad -\frac{1}{2}\int_0^{\frac{2\pi}{L_s}} d\phi \int_0^{2\pi} d\theta \frac{\boldsymbol{j_p}\cdot\boldsymbol{B}}{B^2} h_s\sqrt{g}\boldsymbol{B}\cdot\boldsymbol{\nabla}(\xi^s)^2\end{aligned}$$

STABILITY STUDIES FOR LHD

- Fixed boundary LHD equilibrium computed with ANIMEC with vacuum magnetic axis at $R_{ax} = 3.5m$ and vanishing toroidal current.
- The experimental results reported have $\langle \beta_{dia} \rangle \sim 5\%$ and $\langle \beta_{th} \rangle \sim 3.5\%$. It is assumed that the hot particles are isotropically distributed in velocity space.
- Examine stability properties if $p_{||} \neq p_{\perp}$.
- Profile choices:
  - Thermal pressure: $p(s) = p(0)(1-s)(1-s^4)$,
  - Hot particle pressure: $p_h(s) = p_h(0)(1-s)$,
  - Effective toroidal current: $2\pi J(s) = 0$
  - $T_{||}/T_{\perp} = const.$ varied between $1/3$ and 3.
- The coefficients $p(0)$ and $p_h(0)$ adjusted to maintain $\langle \beta_{dia} \rangle \sim 5\%$ and $\langle \beta_{th} \rangle \sim 3.5\%$.

EQUILIBRIUM PROPERTIES

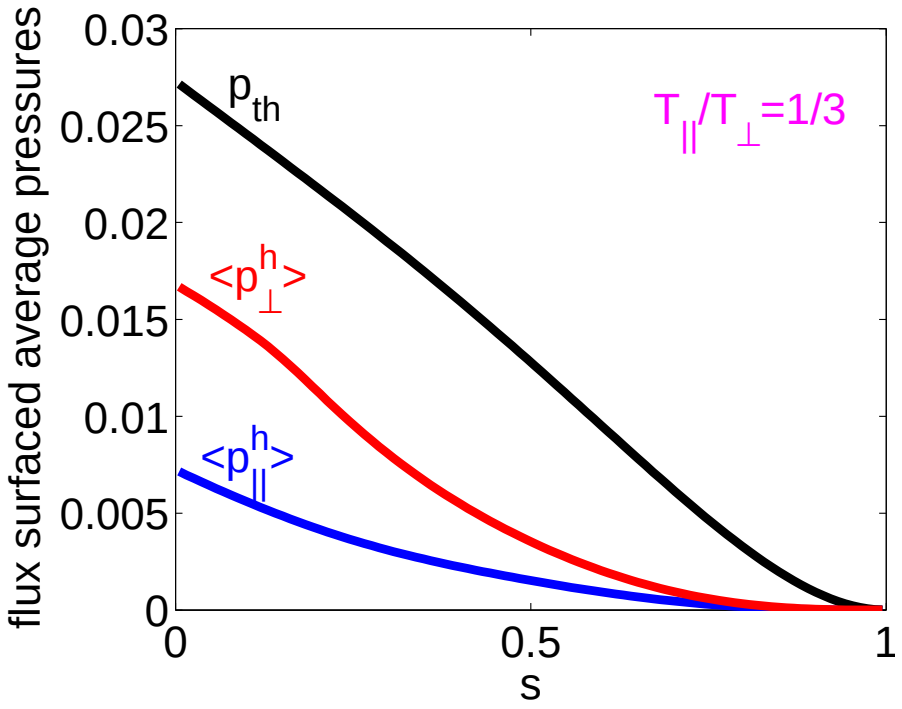

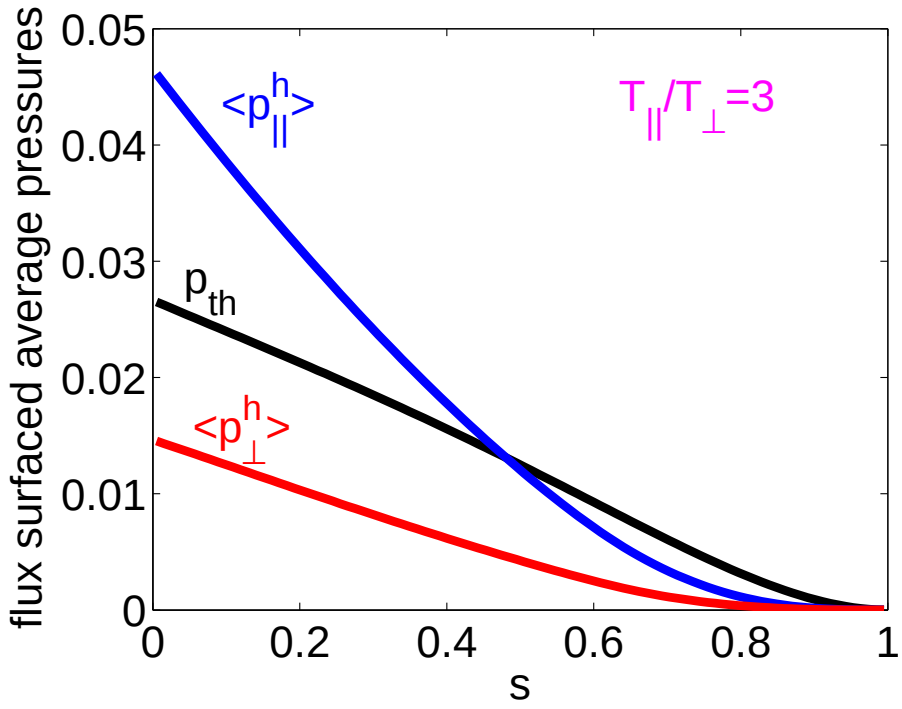

- The flux surface averaged pressure profiles for $T_{||}/T_{\perp} = 1/3$ (left) and for $T_{||}/T_{\perp} = 3$ (right).

EQUILIBRIUM PROPERTIES

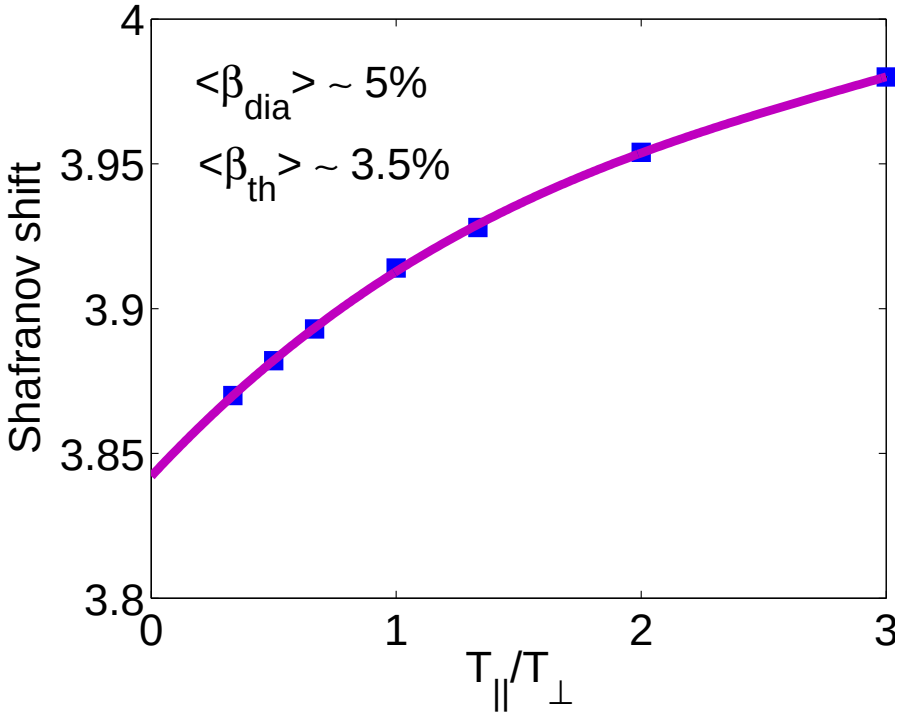

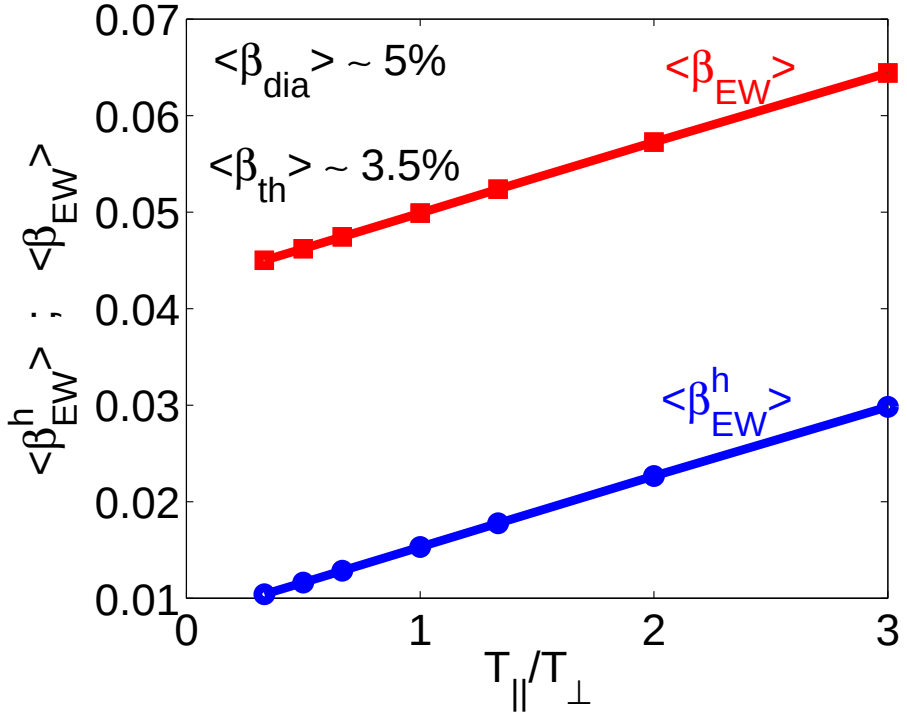

- The Shafranov shift as a function of $T_{||}/T_\perp$ at fixed $\langle\beta_{dia}\rangle \sim 5\%$ (left).
- $\langle\beta_{EW}\rangle$ and $\langle\beta^h_{EW}\rangle$ as a function of $T_{||}/T_\perp$ where $\beta^h_{EW} \equiv (\beta^h_{||} + \beta^h_\perp)/2$ and $\beta_{EW} \equiv \beta_{th} + \beta^h_{EW}$ (right).

EQUILIBRIUM PROPERTIES

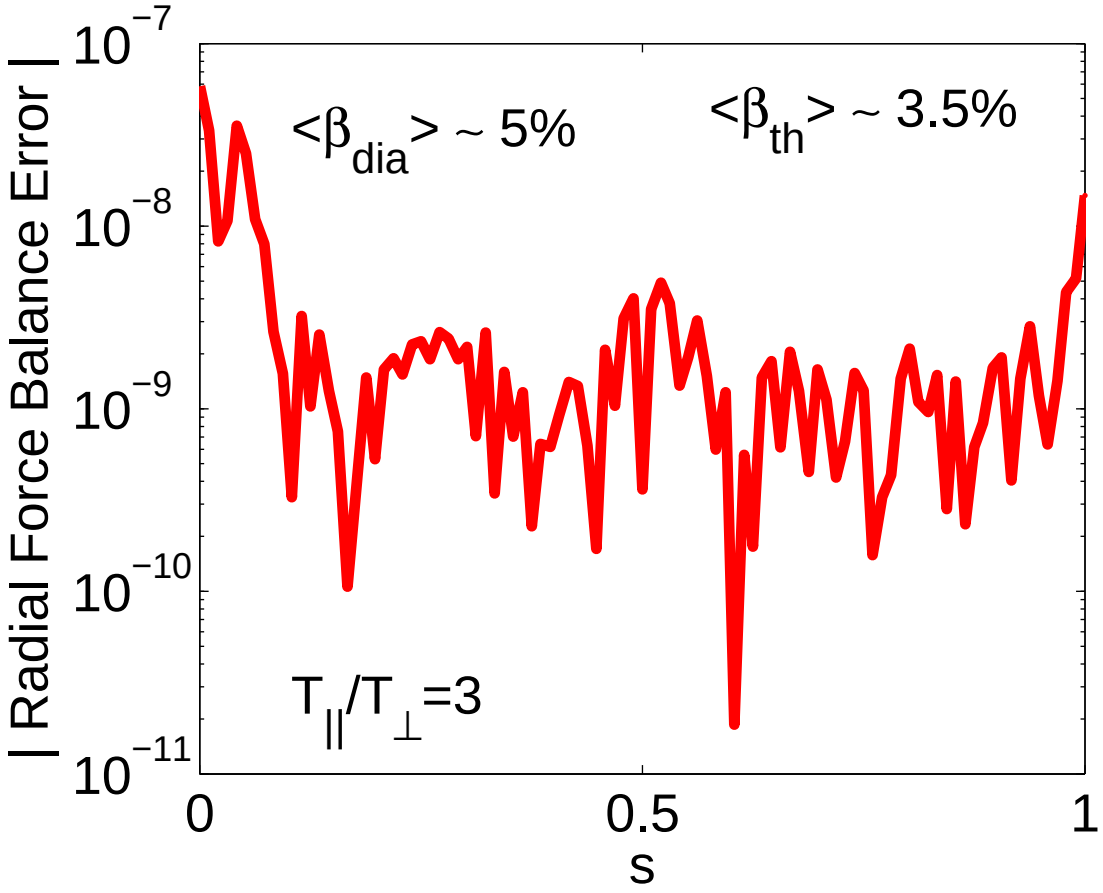

- The profile of the absolute value of the flux surface averaged force balance error.

EQUILIBRIUM PROPERTIES

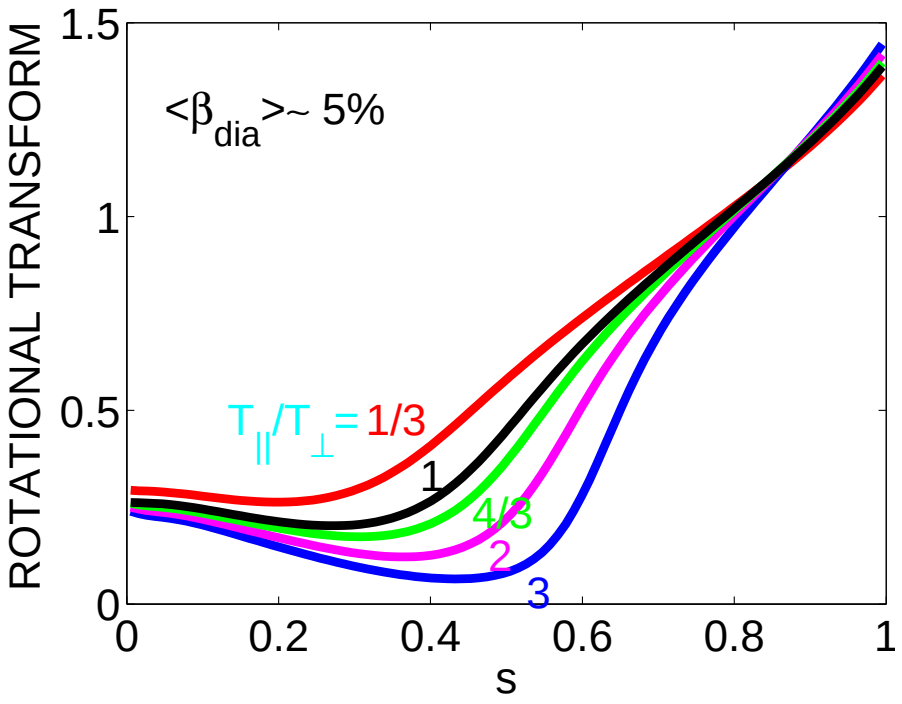

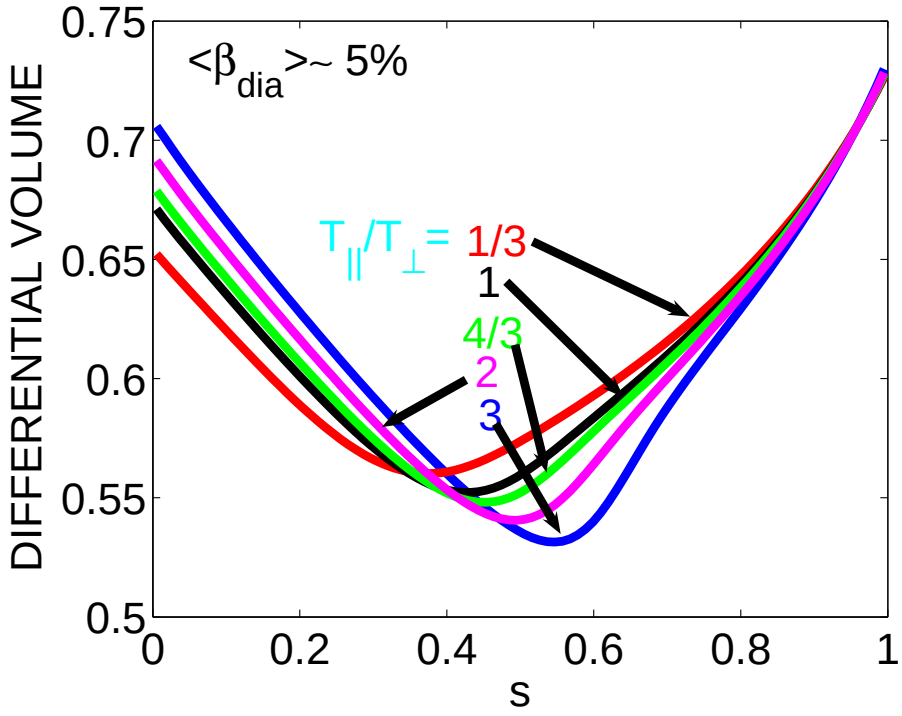

- The LHD rotational transform profiles for different values of $T_{||}/T_{\perp}$ at fixed $\langle\beta_{dia}\rangle \sim 5\%$ and $\langle\beta_{th}\rangle \sim 3.5\%$ (left).
- The LHD differential volume profiles for different values of $T_{||}/T_{\perp}$ at fixed $\langle\beta_{dia}\rangle \sim 5\%$ and $\langle\beta_{th}\rangle \sim 3.5\%$ (right).

GLOBAL STABILITY PROPERTIES

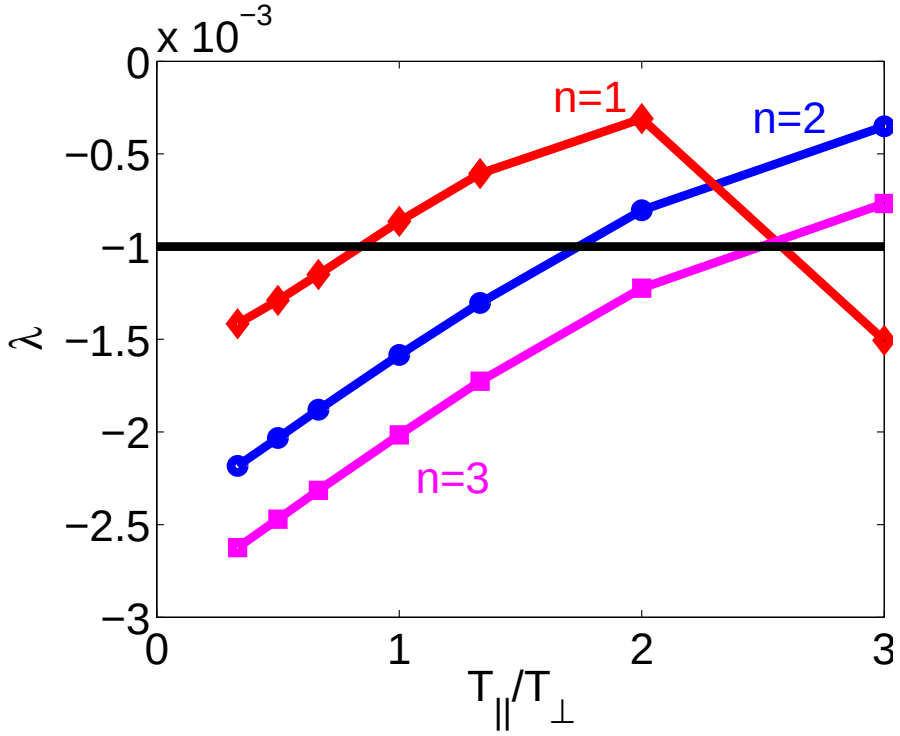

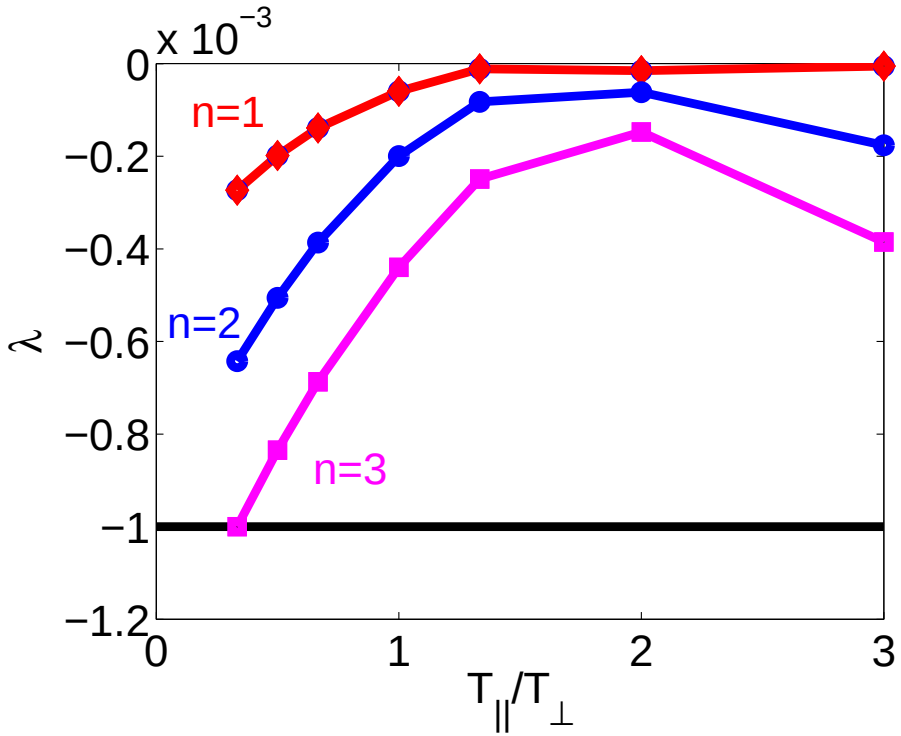

- The eigenvalues as a function of $T_{||}/T_{\perp}$ at fixed $\langle\beta_{dia}\rangle \sim 5\%$ and $\langle\beta_{th}\rangle \sim 3.5\%$ for the the $n = 1$, $n = 2$ and $n = 3$ families of modes according to the fully interacting KO model (left) and the rigid noninteracting model (right).

GLOBAL STABILITY PROPERTIES

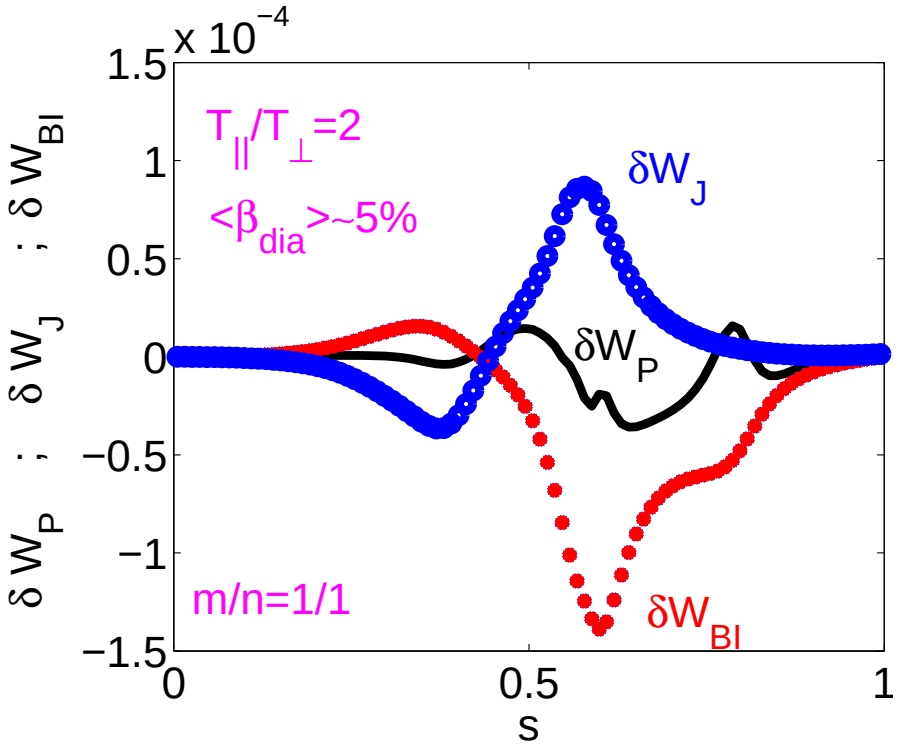

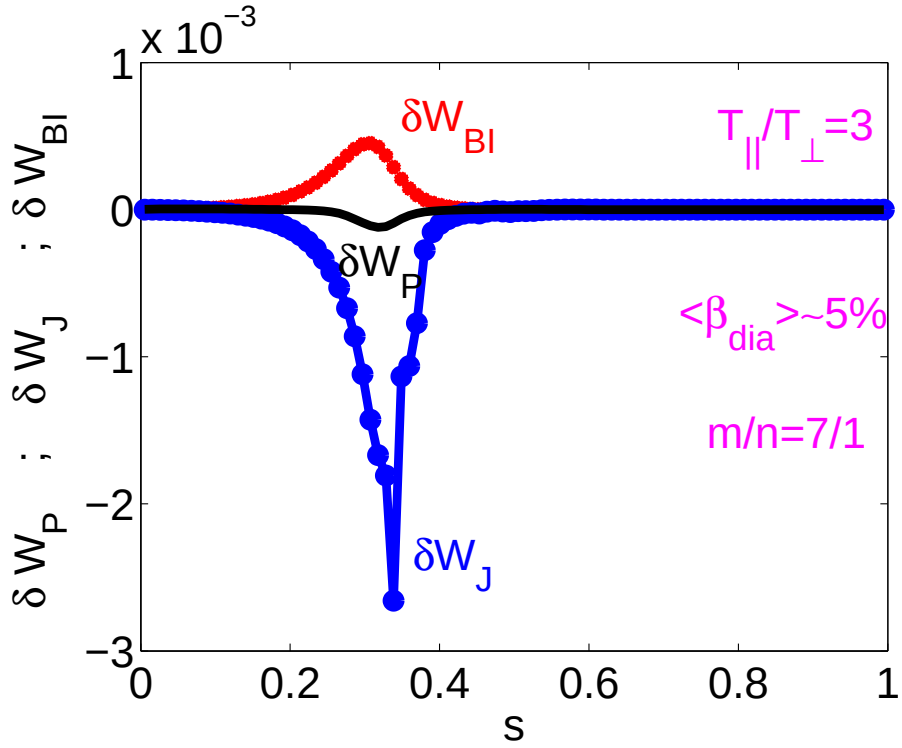

- The profiles of the flux surface averaged perturbed energy components δW_P, δW_{BI} and δW_J at fixed $\langle \beta_{dia} \rangle \sim 5\%$ and $\langle \beta_{th} \rangle \sim 3.5\%$ for $T_{||}/T_\perp = 2$ (left) and for $T_{||}/T_\perp = 3$ (right) according to the fully interacting KO model for the $n = 1$ family of modes.

GLOBAL STABILITY PROPERTIES

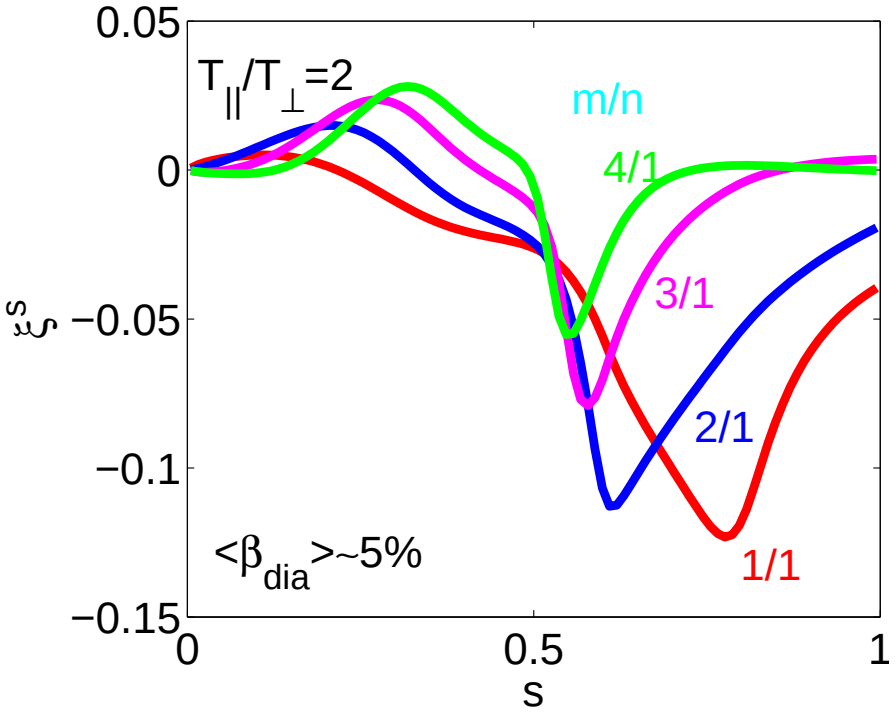

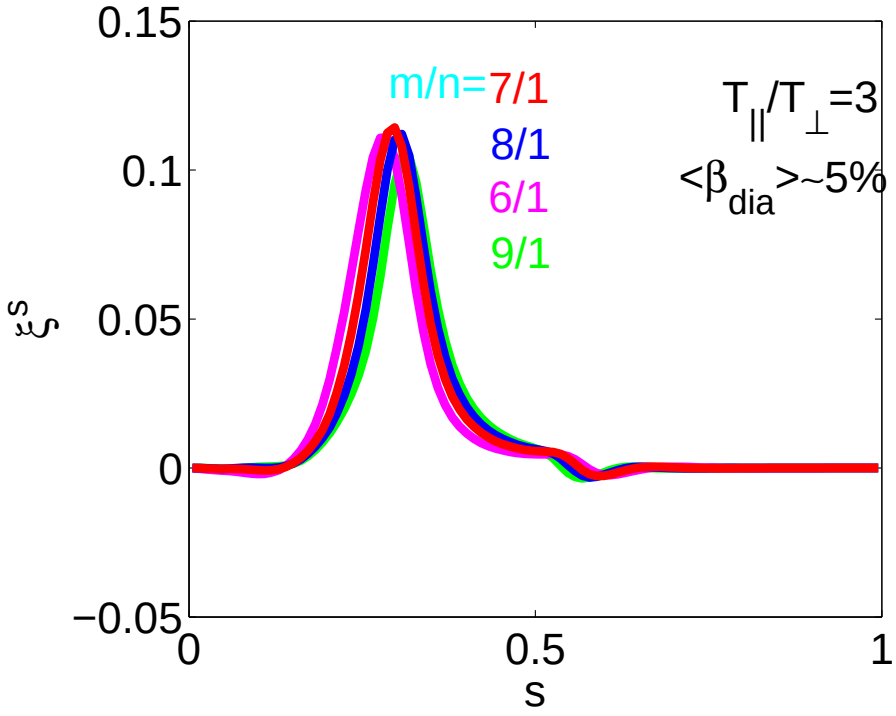

- The profiles of the 5 dominant mode pairs of the radial component of the perturbed displacement vector ξ^s due to the $n = 1$ family for $T_{||}/T_\perp = 2$ (left) and for $T_{||}/T_\perp = 3$ (right) according to the fully interacting KO model.

BEAM DRIVEN FUSION IN HELIOTRON

- As LHD has achieved stable operation at $\langle \beta_{dia} \rangle \sim 5\%$ using high power tangential injection, the prospect of a beam-driven fusion system with large $\langle \beta_{||} \rangle$ becomes a very relevant option to explore particularly with consideration to advanced fuel cycles.

- Apply same configuration as LHD but with large $\left\langle \beta_{||}^{h} \right\rangle$ to examine equilibrium and fluid stability properties.

- Profile choices:
  - Thermal pressure: $p(s) = p(0)(1-s)(1-s^4)$,
  - Hot particle pressure: $p_h(s) = p_h(0)(1-s)$,
  - Effective toroidal current: $2\pi J(s) = 0$
  - $T_{||}/T_{\perp} = 10$

- The coefficient $p(0)$ is adjusted to maintain $\langle \beta_{th} \rangle \sim 1\%$ and $p_h(0)$ varies $\left\langle \beta_{||}^{h} \right\rangle$.

EQUILIBRIUM PROPERTIES

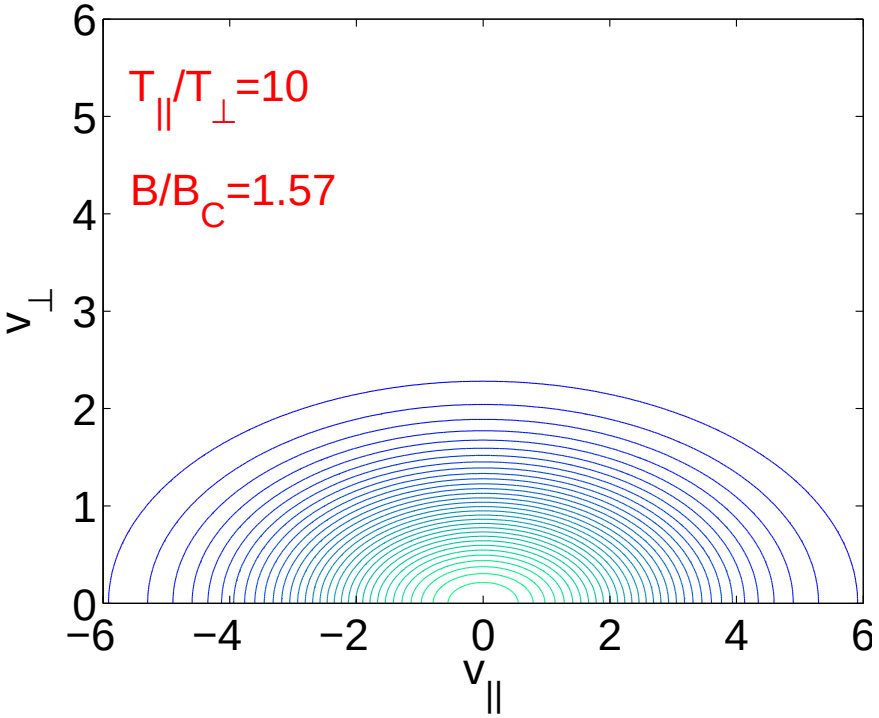

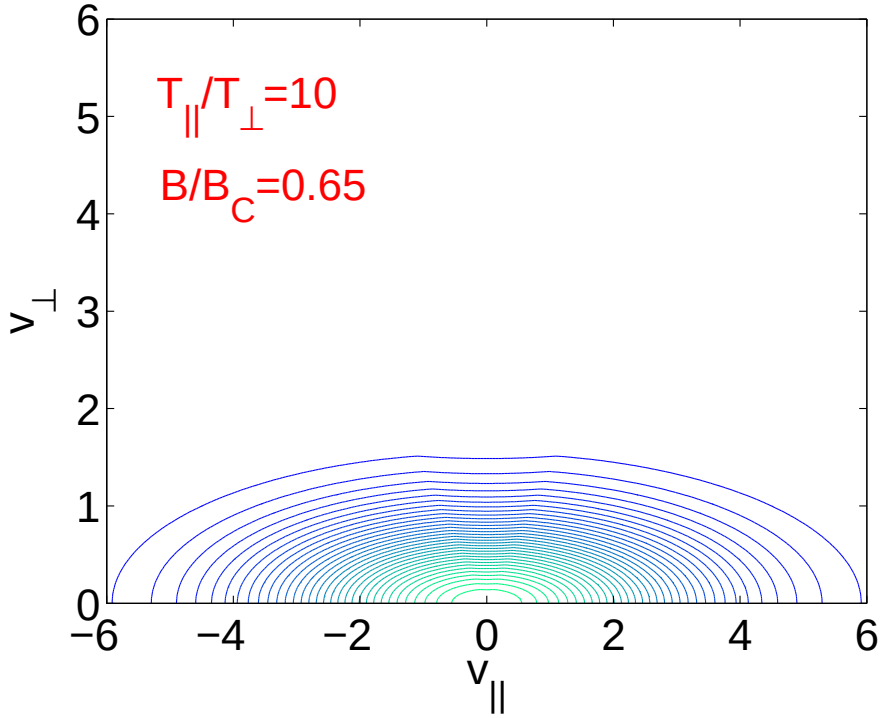

- Contours of the hot particle distribution function from the Bi-Maxwellian model on the high field side ($B/B_C = 1.57$) (left) and on the low field side($B/B_C = 0.65$) for (right).

EQUILIBRIUM PROPERTIES

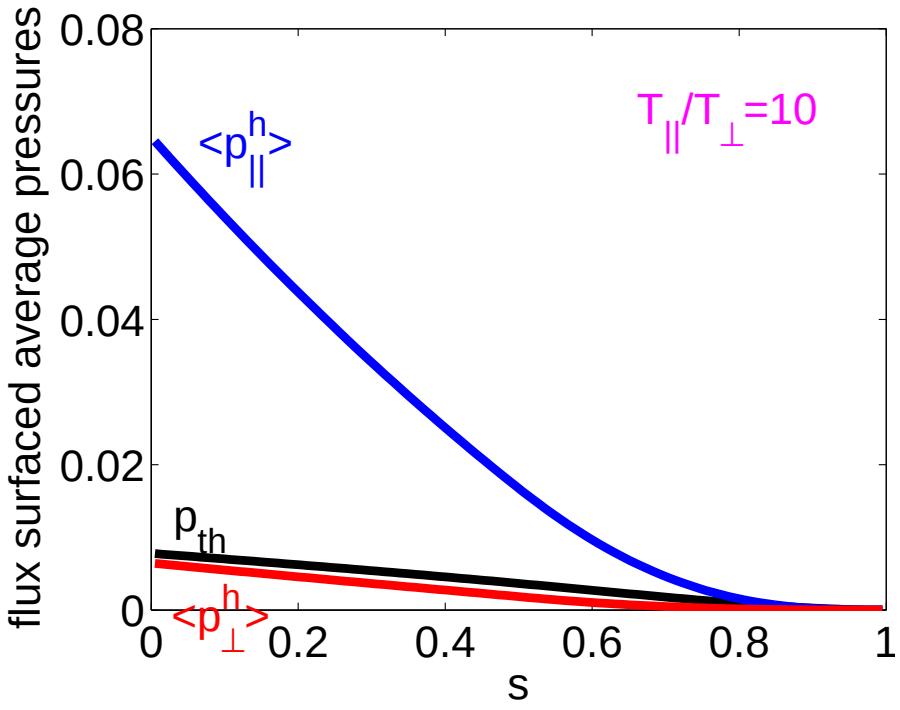

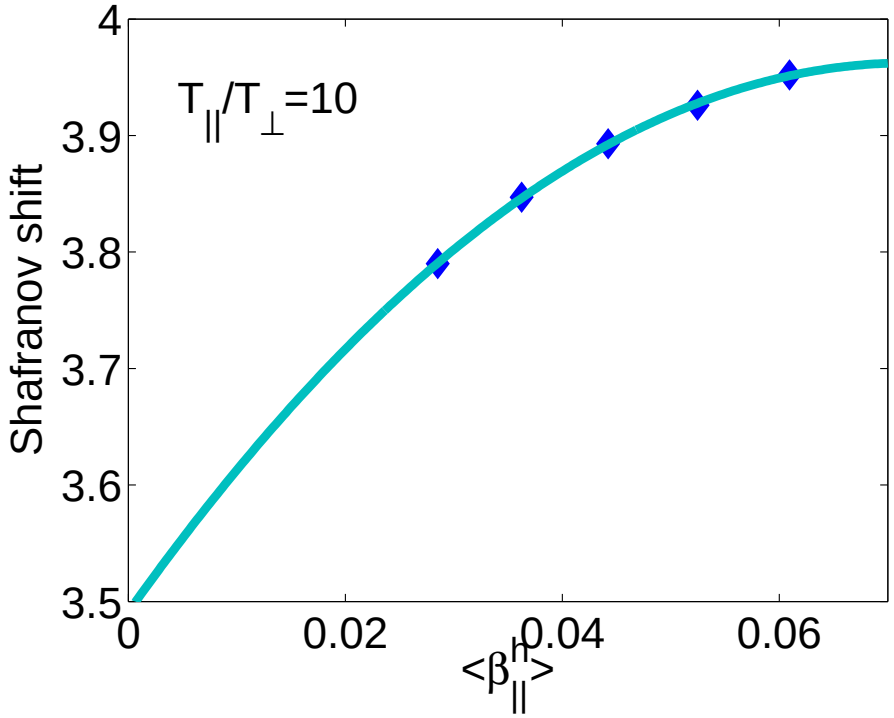

- The flux surface averaged pressure profiles for $T_{||}/T_{\perp} = 10$ (left) and the Shafranov shift as a function of $\left\langle \beta_{||}^{h} \right\rangle$ for $\langle \beta_{th} \rangle \sim 1\%$ (right).

EQUILIBRIUM PROPERTIES

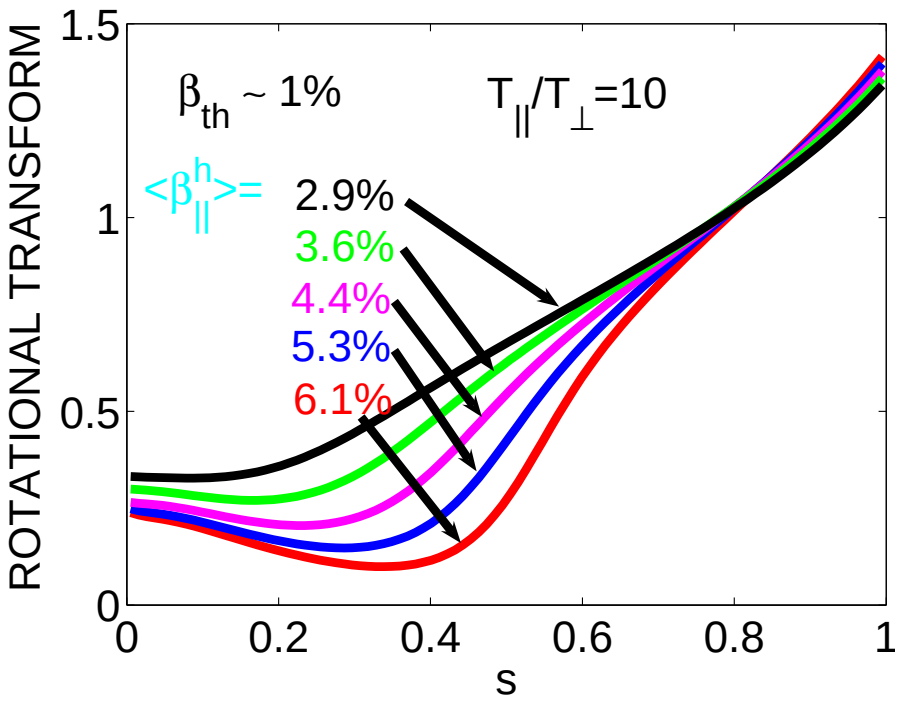

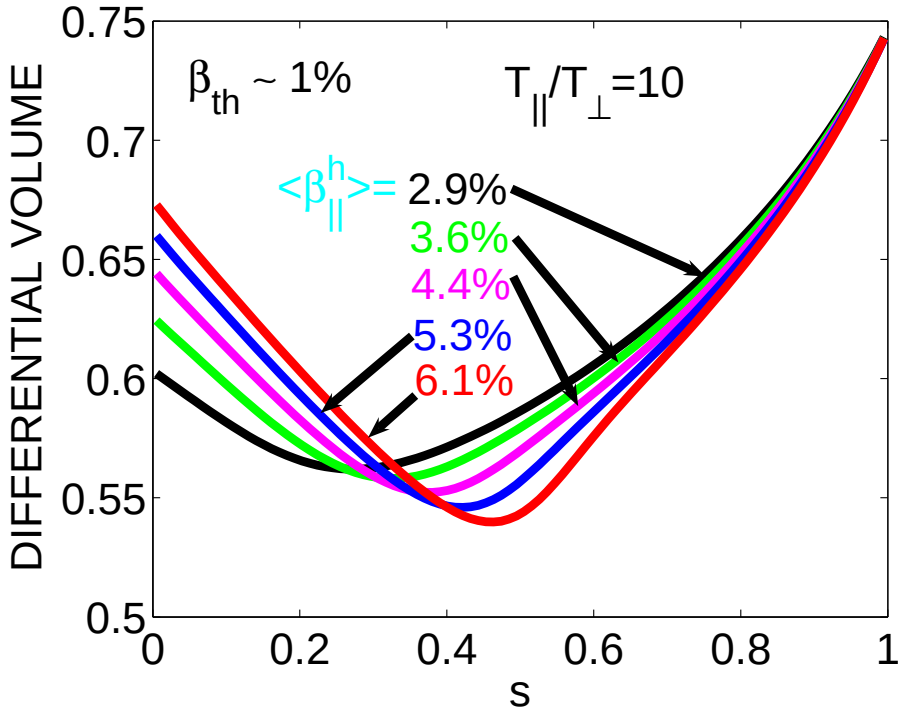

- The rotational transform profiles for different values of $\left\langle \beta_{||}^{h} \right\rangle$ at fixed $T_{||}/T_{\perp} = 10$ and $\langle \beta_{th} \rangle \sim 1\%$ (left).
- The differential volume profiles for different values of $\left\langle \beta_{||}^{h} \right\rangle$ at fixed $T_{||}/T_{\perp} = 10$ and $\langle \beta_{th} \rangle \sim 1\%$ (right).

GLOBAL STABILITY PROPERTIES

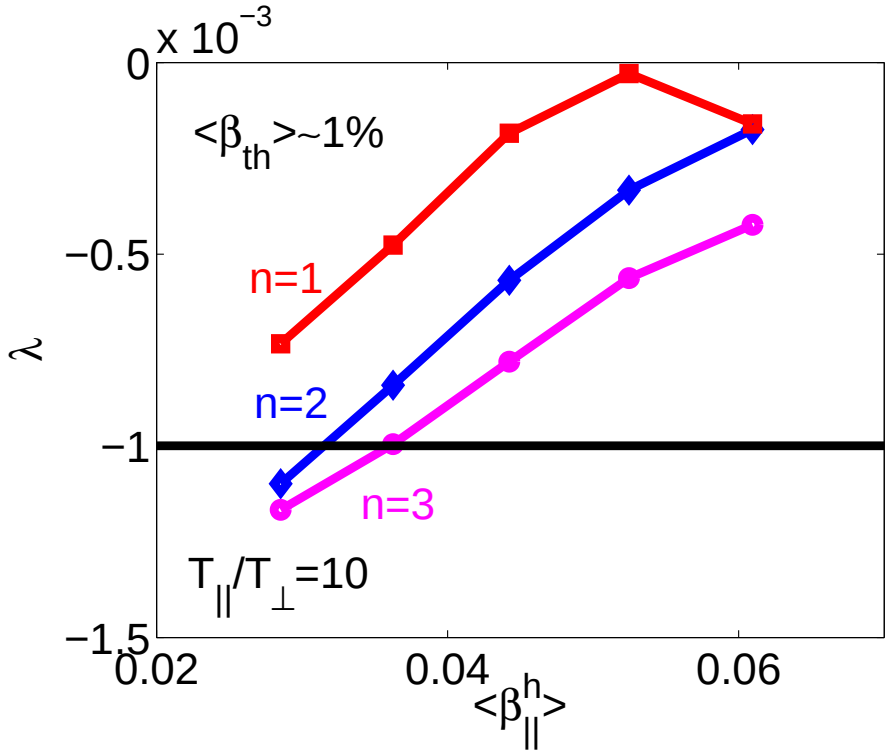

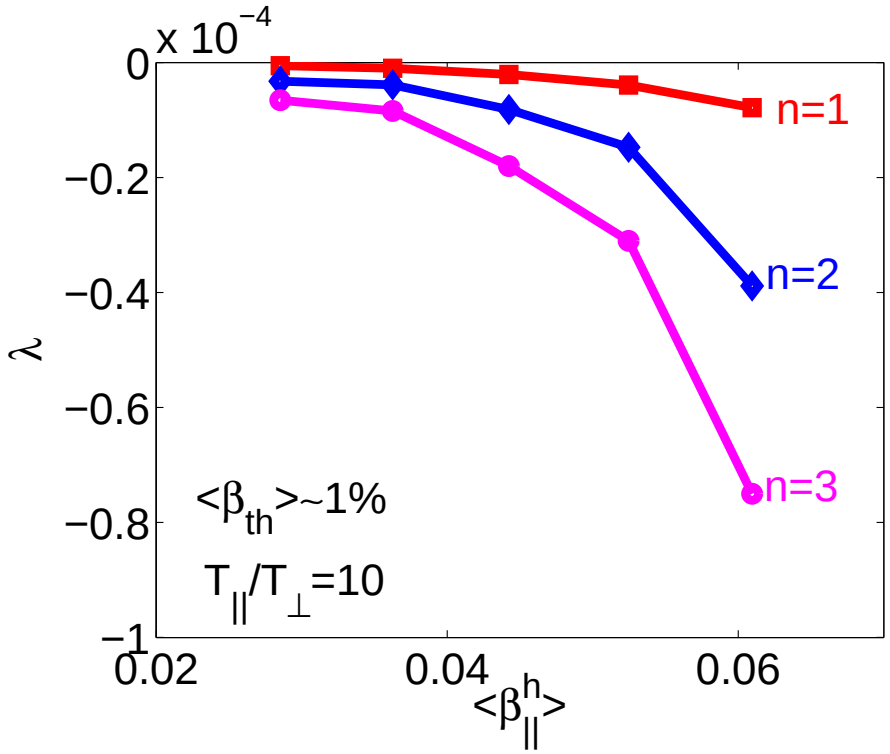

- The eigenvalues as a function of $\left\langle \beta_{||}^{h} \right\rangle$ at fixed $T_{||}/T_{\perp} = 10$ and $\langle \beta_{th} \rangle \sim 1\%$ for the the $n = 1$, $n = 2$ and $n = 3$ families of modes according to the fully interacting KO model (left) and the rigid noninteracting model (right).

GLOBAL STABILITY PROPERTIES

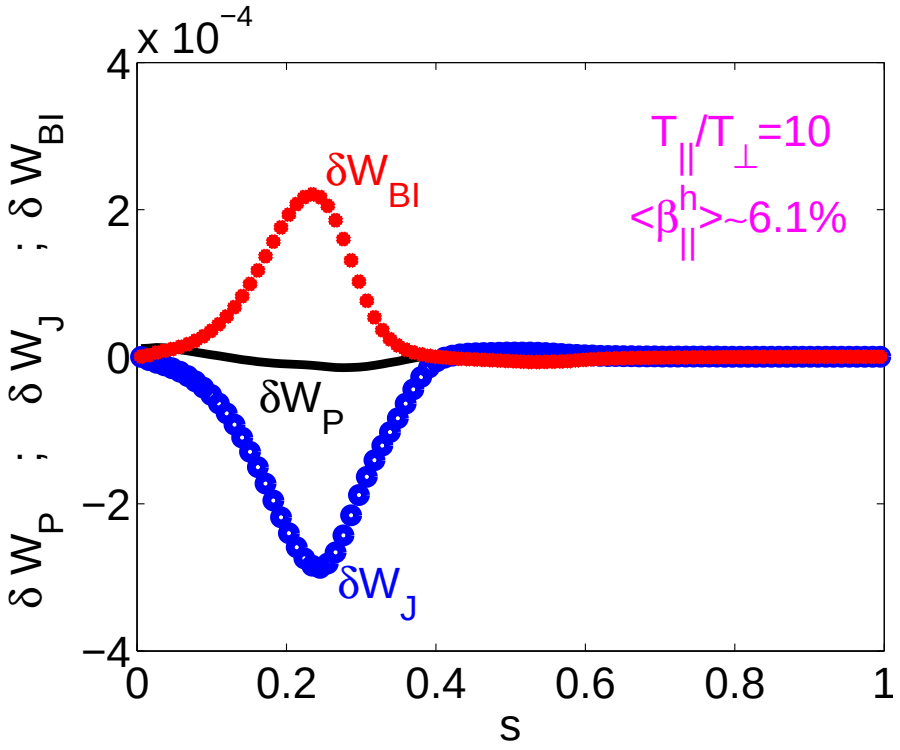

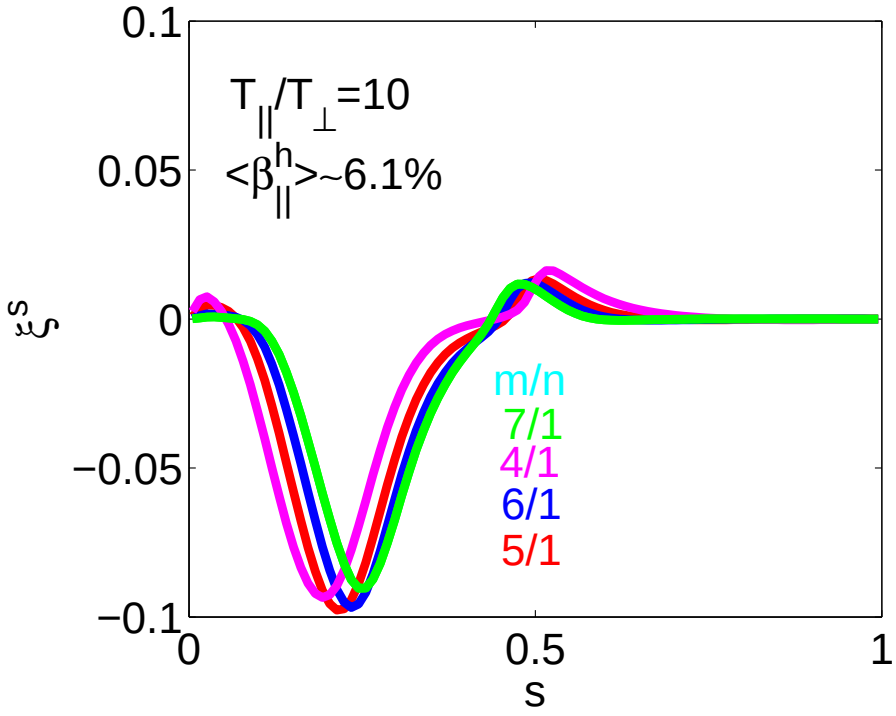

- The profiles of the flux surface averaged perturbed energy components δW_P, δW_{BI} and δW_J associated with the $n = 1$ mode family according to the fully interacting KO model. at fixed $T_{||}/T_\perp = 10$ and $\left\langle \beta^h_{||} \right\rangle \sim 6.1\%$ (left).
- The profiles of the 5 dominant mode pairs of the radial component of the perturbed displacement vector ξ^s due to the $n = 1$ mode family according to the fully interacting KO model. for $T_{||}/T_\perp = 10$ and $\left\langle \beta^h_{||} \right\rangle \sim 6.1\%$ (right).

Conclusions for Equilibrium Studies

- We have developed the ANIMEC code by adapting the free boundary 3D VMEC2000 code to compute anisotropic pressure equilibria based on a variant of a Bi-Maxwellian distribution function for the energetic particles that satisfies the constraint $\boldsymbol{B} \cdot \boldsymbol{\nabla} \mathcal{F}_h = 0$.
- The applications have concentrated on off-axis high-field and low-field energetic particle deposition in a 2-field period quasiaxisymmetric stellarator reactor system.
- The equilibrium calculation recovers vacuum flux surfaces obtained from Poincaré plots resulting from magnetic field line ray tracing.
- For $p_{\|} > p_{\perp}$, the hot particle pressure contours do not differ significantly whether high-field or low-field deposition is applied and the pressures remain more or less uniform on a flux surface.

Conclusions for Equilibrium Studies

- For $p_\perp > p_\parallel$, the energetic particle perpendicular pressure contours concentrate in the region of deposition, for example on the high field side for high field deposition. This can be understood by the fact that the trapped hot particles spend most of their time around the deposition region locally enhancing the perpendicular pressure.
- For $p_\perp > p_\parallel$, the energetic particle parallel pressure contours localise in the low-field region.

Conclusions for LHD Stability Studies

- The global stability of LHD equilibria have been investigated for a sequence with fixed $\langle\beta_{dia}\rangle \sim 5\%$ and $\langle\beta_{th}\rangle \sim 3.5\%$ varying the hot particle temperature ratio in the range $1/3 \leq T_{||}/T_{\perp} \leq 3$. An equilibrium limit is reached for $T_{||}/T_{\perp} > 3$.
- The fully interacting KO model shows that weakly unstable eigenvalues become stabilised with increasing $T_{||}/T_{\perp}$ for the $n = 1$, $n = 2$ and $n = 3$ mode families.
- However, the $n = 1$ mode family is detabilised for $T_{||}/T_{\perp} > 2$ associated with a transition from a virtually stable external ballooning-interchange driven structure to a weakly unstable internal kink mode.
- The optimal stability properties according to the KO model are realised for $2 < T_{||}/T_{\perp} < 3$. The NI model predicts only very weak instability structures.

Conclusions for Beam-Driven Fusion System

- An equilibrium limit is hit when $\left\langle \beta_{||}^{h} \right\rangle \sim 6.1\%$ at $\langle \beta_{th} \rangle \sim 1\%$.
- The eigenvalues for the $n = 1$, $n = 2$ and $n = 3$ mode families become more stable with increasing $\left\langle \beta_{||}^{h} \right\rangle$ and fall within the bounds of σ-stability ($\lambda > -1 \times 10^{-3}$) for $T_{||}/T_{\perp} > 3$ according to the KO fully interacting model.
- The $n = 1$ mode family structure at $\left\langle \beta_{||}^{h} \right\rangle \sim 6.1\%$ corresponds to an internal kink mode.
- Basic estimates: For $\langle \beta_{th} \rangle = 1\%$, $\left\langle \beta_{||}^{h} \right\rangle = 6\%$, $N_e = 1 \times 10^{19}/m^3$, $T_{||} = 500keV$ and $B_0 = 0.8T$ we get $T_e \simeq 1.8keV$ and $N_h \simeq 2 \times 10^{17}/m^3$.